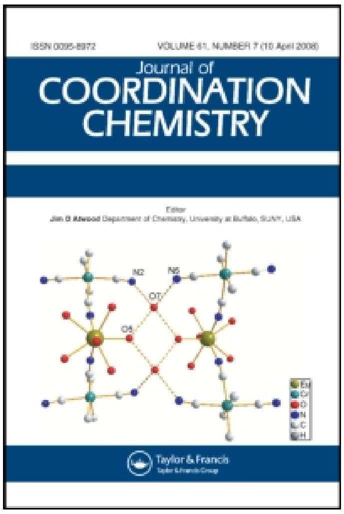

Journal of Coordination Chemistry

Publication details, including instructions for authors and subscription information:
http://www.informaworld.com/smpp/title~content=t713455674

Synthesis, spectroscopic, and thermal analyses of trinuclear Mn(II), Co(II), Ni(II), and Zn(II) complexes with some sulfa derivatives

Abdalla M. Khedr[a]; Dooa F. Draz[a]
[a] Faculty of Science, Department of Chemistry, Tanta University, Tanta, Egypt

To cite this Article Khedr, Abdalla M. and Draz, Dooa F.(2010) 'Synthesis, spectroscopic, and thermal analyses of trinuclear Mn(II), Co(II), Ni(II), and Zn(II) complexes with some sulfa derivatives', Journal of Coordination Chemistry, 63: 8, 1418 — 1429, First published on: 13 April 2010 (iFirst)

To link to this Article: DOI: 10.1080/00958971003774241

URL: http://dx.doi.org/10.1080/00958971003774241

Journal of Coordination Chemistry
Vol. 63, No. 8, 20 April 2010, 1418–1429

Synthesis, spectroscopic, and thermal analyses of trinuclear Mn(II), Co(II), Ni(II), and Zn(II) complexes with some sulfa derivatives

ABDALLA M. KHEDR* and DOOA F. DRAZ

Faculty of Science, Department of Chemistry, Tanta University, Tanta, Egypt

(*Received 28 September 2009; in final form 23 December 2009*)

New bi- and trihomonuclear Mn(II), Co(II), Ni(II), and Zn(II) complexes with sulfa-guanidine Schiff bases have been synthesized for potential chemotherapeutic use. The complexes are characterized using elemental and thermal (TGA) analyses, mass spectra (MS), molar conductance, IR, ^{1}H-NMR, UV-Vis, and electron spin resonance (ESR) spectra as well as magnetic moment measurements. The low molar conductance values denote non-electrolytes. The thermal behavior of these chelates shows that the hydrated complexes lose water of hydration in the first step followed by loss of coordinated water followed immediately by decomposition of the anions and ligands in subsequent steps. IR and ^{1}H-NMR data reveal that ligands are coordinated to the metal ions by two or three bidentate centers *via* the enol form of the carbonyl C=O group, enolic sulfonamide S(O)OH, and the nitrogen of azomethine. The UV-Vis and ESR spectra as well as magnetic moment data reveal that formation of octahedral $[Mn_2L^1(AcO)_2(H_2O)_6]$ (**1**), $[Co_2(L^1)_2(H_2O)_8]$ (**2**), $[Ni_2L^1(AcO)_2(H_2O)_6]$ (**3**), $[Mn_3L^2(AcO)_3(H_2O)_9]$ (**5**), $[Co_3L^2(AcO)_3(H_2O)_9]\cdot 4H_2O$ (**6**), $[Ni_3L^2(AcO)_3(H_2O)_9]\cdot 7H_2O$ (**7**), $[Mn_3L^3(AcO)_3(H_2O)_6]$ (**9**), $[Co_2(HL^3)_2(H_2O)_8]\cdot 4H_2O$ (**10**), $[Ni_3L^3(AcO)_3(H_2O)_9]$ (**11**), $[Mn_3L^4(AcO)_3(H_2O)_9]\cdot H_2O$ (**13**), $[Co_2(HL^4)_2(H_2O)_8]\cdot 5H_2O$ (**14**), and $[Ni_3L^4(AcO)_3(H_2O)_9]$ (**15**) while $[Zn_2L^1(AcO)_2(H_2O)_2]$ (**4**), $[Zn_3L^2(AcO)_3(H_2O)_3]\cdot 2H_2O$ (**8**), $[Zn_3L^3(AcO)_3(H_2O)_3]\cdot 3H_2O$ (**12**), and $[Zn_3L^4(AcO)_3(H_2O)_3]\cdot 2H_2O$ (**16**) are tetrahedral. The electron spray ionization (ESI) MS of the complexes showed isotope ion peaks of $[M]^+$ and fragments supporting the formulation.

Keywords: Bi- and trihomonuclear Mn(II), Co(II), Ni(II), and Zn(II) complexes; Sulfa-guanidine based ligands

1. Introduction

Sulfonamides were the first effective chemotherapeutic agents employed systematically for the prevention and cure of bacterial infections in humans [1, 2]. The vast commercial success of these medicinal agents has made the chemistry of sulfonamides a major area of research and an important branch in pharmaceutical sciences [3]. Complex formation between metal ions and sulfa drugs, combining antibacterial activity of sulfonamides and microbial activity of the metal ions, constitute an important field of research. Metal complexes of Schiff bases derived from sulfa drugs have gained considerable

---

*Corresponding author. Email: abkhedr2001@yahoo.com

Journal of Coordination Chemistry
ISSN 0095-8972 print/ISSN 1029-0389 online © 2010 Taylor & Francis
DOI: 10.1080/00958971003774241

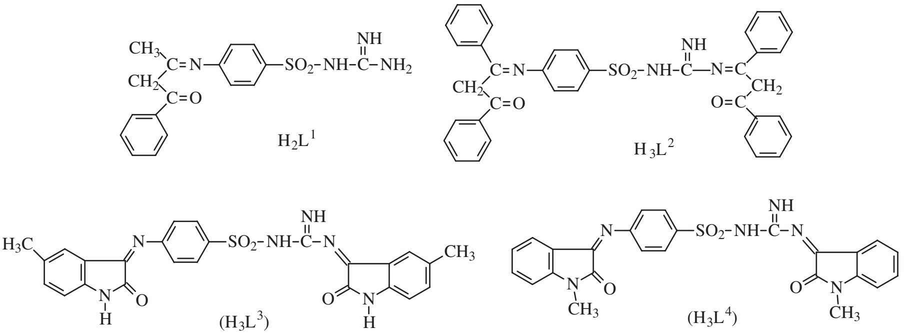

Figure 1. Structures of the prepared sulfa-guanidine Schiff bases.

importance due to their pronounced antimicrobial and fungicidal activities [3–7]. Polynuclear metal ion complexes usually have peculiar spectroscopic and magnetic properties [8–11], besides wide applications in biological systems, catalysis, and material science [12–14]. In view of the bioinorganic and medicinal importance of such complexes, it was thought worthwhile to synthesize and characterize some bi- and trihomonuclear Mn(II), Co(II), Ni(II), and Zn(II) complexes with Schiff bases derived from condensation of sulfa-guanidine and 1-benzoylacetone (H_2L^1), dibenzoylmethane (H_3L^2), 5-methylisatine (H_3L^3), or 1-methylisatine (H_3L^4) (figure 1).

2. Experimental

All chemicals used were of analytical reagent grade and used as supplied.

2.1. *Synthesis of sulfa-guanidine Schiff bases*

Schiff bases of sulfa-guanidine were prepared as follows: a methanolic solution (20 mL) of sulfa-guanidine (2.14 g, 10 mmol) was added to the solution (≈20 mL) of 1-benzoylacetone (1.60 g, 10 mmol), dibenzoylmethane (4.49 g, 20 mmol), 5-methylisatine (3.22 g, 20 mmol) or 1-methylisatine (3.22 g, 20 mmol) in methanol. The resulting solution was refluxed with stirring for 8–9 h and then filtered to remove insoluble content. The filtrate so obtained was concentrated on a water bath and left overnight at room temperature; colored crystals of the Schiff bases separated from their respective solutions were filtered off and purified by repeated recrystallization from the appropriate solvent (yield 75–80%) [15].

2.2. *Synthesis of the complexes*

The following general procedure was used in the synthesis of all metal complexes. The salts, $(CH_3CO_2)_2Mn \cdot 2H_2O$ (2.68 g, 10 mmol), $(CH_3CO_2)_2Co \cdot 4H_2O$ (1.99 g, 10 mmol), $(CH_3CO_2)_2Ni \cdot 4H_2O$ (2.49 g, 10 mmol), or $(CH_3CO_2)_2Zn \cdot 2H_2O$ (2.20 g, 10 mmol) were dissolved in water (20 mL) and the solution was added to a warmed, stirred methanolic solution (≈30 mL) of the corresponding Schiff bases H_2L^1 (1.79 g, 5 mmol), H_3L^2 (1.88 g, 3 mmol), H_3L^3 (1.50 g, 3 mmol), or H_3L^4 (1.50 g, 3 mmol). The mixture was left under reflux with continuous stirring for 8 h and the solid complexes precipitated. The resulting solid was filtered off, washed several times with methanol, and dried in vacuum over anhydrous calcium chloride.

2.3. *Physical methods*

Microanalyses (C, H, and N) of the prepared complexes were performed in the Microanalytical Center, Tanta University. Electron spray ionization (ESI) mass spectra (MS) were recorded on a Shimadzu LCMS-2010 eV spectrometer at the Gakushuin University (Japan). The molar conductance of solid complexes in dimethylformamide (DMF) was measured using a conductance bridge of the type 523 conductometer. Thermal gravimetric analysis (TGA) was performed with a Mettler TA4000 system consisting of a TG50 furnace, a M3 microbalance and TA72 graphware in the temperature range 25–800°C at a scanning rate of 10°C min^{-1} under nitrogen with a flow rate of 60 mL min^{-1}. Solid-state infrared spectra were recorded as KBr discs with a Perkin Elmer (model 1430) IR spectrophotometer from 4000 to 200 cm^{-1}. ^{1}H-NMR spectra were measured on a JEOL JNM-AL 300 (300 MHz) spectrometer. UV-Vis spectra were recorded on a Shimadzu UV-Vis 160A spectrophotometer with a rectangular quartz cell of dimensions 0.2×1 cm from 200 to 900 nm in our laboratory. Magnetic measurements were performed by Gouy's method using magnetic susceptibility instrument (20 KG) at room temperature. Molar susceptibilities were corrected for diamagnetism of the component atoms applying Pascal's constants. Room temperature X-band powder electron spin resonance (ESR) spectra of the complexes were recorded using a Jeol spectrometer model JES-FE2XG Jeol equipped with an E101 microwave bridge. The magnetic field was calibrated with dipicrylhydrazyl. Chemical shifts of ^{1}H-NMR was expressed in parts per million (ppm, δ units) and coupling constant was expressed in units of hertz (Hz). The samples were dissolved in DMSO-d_6 using tetramethylsilane as internal reference. Metal contents were determined complexometrically using standard ethylenediamine tetraacetic acid (EDTA) titration [16].

3. Results and discussion

The sulfa-guanidine based ligands (H_2L^1, H_3L^2, H_3L^3, and H_3L^4) were prepared and purified by recrystallization several times from the appropriate solvent until constant melting point. The purity of the ligands was confirmed by elemental and spectral analyses which gave a good agreement with the suggested molecular formulae (figure 1) [17].

3.1. *Elemental analysis, MS, and molar conductance data*

Elemental analyses (C, H, N, and metal content) of **1**–**16** with their molecular formulae are presented in table 1. The constitution and purity of the metal complexes are established by ESI–mass spectrometry. The MS of **1**–**16** showed the highest peaks

Table 1. Elemental analysis and physical properties of the prepared complexes.[a]

Compound No.	Molecular formula (Empirical formula)	Color (Λ_m)	MW from MS (Calcd. M.W)	Elemental analysis Calcd (found) (%) C	H	N	M
1	$[Mn_2L^1(AcO)_2(H_2O)_6]$	Buff	693 (692.46)	36.37	4.94	8.08	15.84
	$(C_{21}H_{34}Mn_2N_4SO_{12})$	(15.3)		(36.49)	(4.66)	(8.32)	(16.31)
2	$[Co_2(L^1)_2(H_2O)_8]$	Faint buff	975	41.89	4.96	11.50	12.09
	$(C_{34}H_{48}Co_2N_8S_2O_{14})$		(974.78)	(42.11)	(4.66)	(11.11)	(12.16)
3	$[Ni_2L^1(AcO)_2(H_2O)_6]$	F. Green	699	36.03	4.32	8.00	16.77
	$(C_{21}H_{30}Ni_2N_4SO_{13})$	(14.6)	(699.98)	(36.51)	(3.99)	(7.69)	(16.33)
4	$[Zn_2L^1(AcO)_2(H_2O)_2]$	Buff	640	39.33	4.09	8.74	20.39
	$(C_{21}H_{26}Zn_2N_4SO_9)$	(14.9)	(641.28)	(39.63)	(4.01)	(8.61)	(20.61)
5	$[Mn_3L^2(AcO)_3(H_2O)_9]$	Brown	1128	46.00	4.83	4.97	15.68
	$(C_{43}H_{54}Mn_3N_4SO_{19})$	(15.5)	(1127.79)	(46.22)	(4.45)	(5.19)	(16.22)
6	$[Co_3L^2(AcO)_3(H_2O)_9] \cdot 4H_2O$	F. Buff	1212	42.62	5.16	4.62	14.59
	$(C_{43}H_{62}Co_3N_4SO_{23})$	(14.9)	(1211.83)	(42.24)	(4.80)	(4.34)	(14.38)
7	$[Ni_3L^2(AcO)_3(H_2O)_9] \cdot 7H_2O$	Postage	1263	40.82	5.42	4.43	13.92
	$(C_{43}H_{68}Co_3N_4SO_{26})$	(15.1)	(1265.19)	(40.76)	(5.76)	(4.69)	(13.87)
8	$[Zn_3L^2(AcO)_3(H_2O)_3] \cdot 2H_2O$	Buff	1083	47.51	4.27	5.15	18.04
	$(C_{43}H_{46}Zn_3N_4SO_{15})$	(14.4)	(1087.06)	(47.71)	(4.66)	(5.44)	(17.82)
9	$[Mn_3L^3(AcO)_3(H_2O)_9]$	Brown	1002	37.18	4.41	8.39	16.46
	$(C_{31}H_{44}Mn_3N_6SO_{19})$	(16.8)	(1001.60)	(37.08)	(4.57)	(8.81)	(16.02)
10	$[Co_2(HL^3)_2(H_2O)_8] \cdot 4H_2O$	Red	1331	45.12	4.54	12.63	8.86
	$(C_{50}H_{60}Co_2N_{12}S_2O_{20})$	(14.1)	(1331.08)	(45.08)	(4.67)	(12.81)	(9.02)
11	$[Ni_3L^3(AcO)_3(H_2O)_9]$	Red	1011	36.76	4.38	8.30	17.39
	$(C_{31}H_{44}Ni_3N_6SO_{19})$	(16.3)	(1012.88)	(37.08)	(4.87)	(8.61)	(17.02)
12	$[Zn_3L^3(AcO)_3(H_2O)_3] \cdot 3H_2O$	Buff	975	38.04	3.91	8.59	20.04
	$(C_{31}H_{38}Zn_3N_6SO_{16})$	(14.2)	(978.88)	(38.08)	(3.57)	(8.81)	(20.02)
13	$[Mn_3L^4(AcO)_3(H_2O)_9] \cdot H_2O$	F. Bown	1020	36.52	4.55	8.24	17.34
	$(C_{31}H_{46}Mn_3N_6SO_{20})$	(15.5)	(1019.61)	(36.48)	(4.57)	(8.51)	(17.42)
14	$[Co_2(HL^4)_2(H_2O)_8] \cdot 5H_2O$	Red	1350	45.52	4.63	12.46	8.74
	$(C_{50}H_{62}Co_2N_{12}S_2O_{21})$	(13.3)	(1349.09)	(45.08)	(4.57)	(12.81)	(9.02)
15	$[Ni_3L^4(AcO)_3(H_2O)_9]$	Brown	1011	36.76	4.38	8.30	17.39
	$(C_{31}H_{44}Ni_3N_6SO_{19})$	(14.5)	(1012.88)	(36.88)	(4.57)	(8.71)	(17.02)
16	$[Zn_3L^4(AcO)_3(H_2O)_3] \cdot 2H_2O$	Buff	957	38.75	3.78	8.75	20.41
	$(C_{31}H_{36}Zn_3N_6SO_{15})$	(15.9)	(960.86)	(38.22)	(3.57)	(8.81)	(20.02)

MW from MS = molecular weight obtained from MS measurements.
(Calcd MW) = calculated molecular weight. Λ_m = molar conductance ($\Omega^{-1}\,cm^2\,mol^{-1}$).
[a] All the synthesized complexes decompose without melting above 220°C.

corresponding to the molecular weights of the proposed formulae based on the atomic weights of ^{55}Mn, ^{59}Co, ^{58}Ni, and ^{64}Zn isotopes; among several molecular weights based on the isotope distribution of the metal [17, 18]. Molecular ion peaks of complexes have been used to confirm the proposed formula (table 1). These assignments are supported by the appearance of molecular species containing the metal as cluster isotope peaks. Such cluster peaks results from the fragmentation of parent molecular ions due to different isotopes of the metals under study [18]. The pattern of the MS gives an impression of the successive degradation of the target compound with the series of peaks corresponding to the various fragments. The spectrum of Ni(II)-complex **3** as an illustrative example under electron impact conditions shows a peak at m/z 358

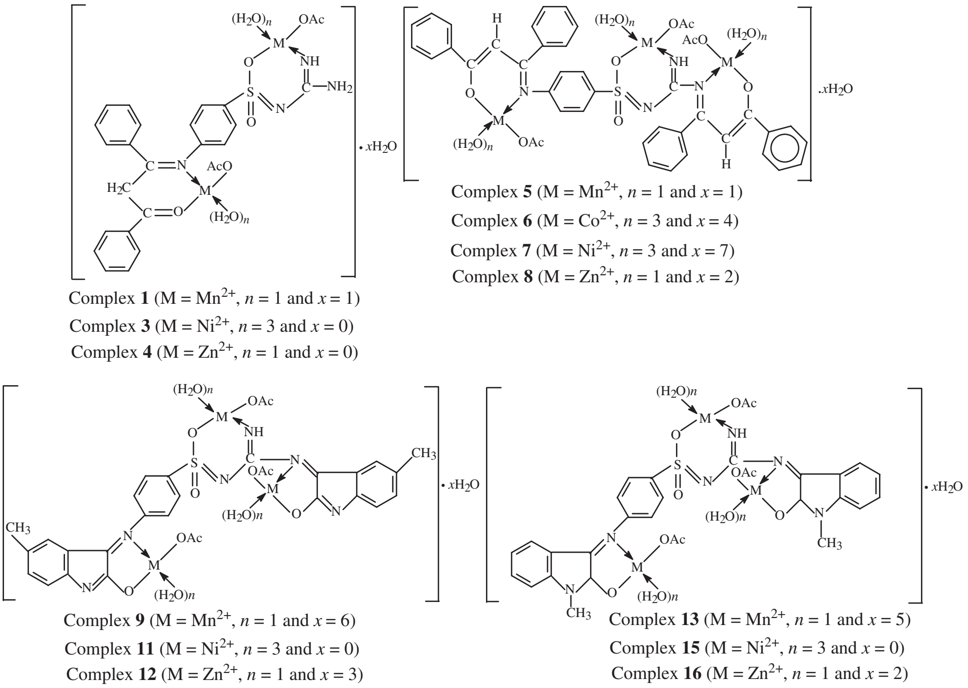

Complex **1** (M = Mn^{2+}, n = 1 and x = 1)
Complex **3** (M = Ni^{2+}, n = 3 and x = 0)
Complex **4** (M = Zn^{2+}, n = 1 and x = 0)

Complex **5** (M = Mn^{2+}, n = 1 and x = 1)
Complex **6** (M = Co^{2+}, n = 3 and x = 4)
Complex **7** (M = Ni^{2+}, n = 3 and x = 7)
Complex **8** (M = Zn^{2+}, n = 1 and x = 2)

Complex **9** (M = Mn^{2+}, n = 1 and x = 6)
Complex **11** (M = Ni^{2+}, n = 3 and x = 0)
Complex **12** (M = Zn^{2+}, n = 1 and x = 3)

Complex **13** (M = Mn^{2+}, n = 1 and x = 5)
Complex **15** (M = Ni^{2+}, n = 3 and x = 0)
Complex **16** (M = Zn^{2+}, n = 1 and x = 2)

Figure 2. The representative structures and mode of bonding in the investigated complexes.

corresponding to molecular ion of H_2L^1 [19]. The spectrum also showed isotope cluster peaks at m/z 699 and 701, at m/z 591 and 593, at m/z 532 and 534, at m/z 473 and 475, at m/z 117, and 119 corresponding to the molecular weights of the complex cation $[Ni_2L^1(AcO)_2(H_2O)_6]^+$, $[Ni_2L^1(AcO)_2]^+$ (loss of coordinated water molecules), $[Ni_2L^1(AcO)]^+$ (loss of coordinated water molecules and one acetate groups), $[Ni_2L^1]^+$ (loss of coordinated water molecules and two acetate groups), nickel acetate radical $Ni(AcO)]^+$, respectively. The most interesting observation for the ESI–MS data of Zn(II) complexes **4**, **8**, **12**, and **16** is the cluster of isotopologue ions of m/z 640, 1083, 975 and 957 (the most intense). Zinc is naturally present as five isotopes; ^{64}Zn: 45.89%, ^{66}Zn: 27.81%, ^{67}Zn: 4.11%, ^{68}Zn: 18.57%, and ^{70}Zn: 0.62% [20] and the magnification of the range of interest clearly confirms the presence of Zn(II) complexes of H_2L^1, H_3L^2, H_3L^3, and H_3L^4 with a distinct pattern of five isotopologue ions with the same distribution and abundances [21]. Molecular ions of **1**–**16** also decompose *via* abstraction of the ligand molecules; metal ion complexes containing different ligands usually decompose during spray ionization through cleavage of the metal-ligand bond. This gives rise to the presence of molecular ion peaks attributable to $[H_nL]^+$ [19]. The results of both elemental analyses and MS are in good agreement with those calculated for the molecular formula of the prepared complexes (figure 2). The DMF solubility of the above complexes made determinations of the molar conductivity (Λ_m) of 10^{-3} mol solution at 25°C possible. The molar conductance (Λ_m, $\Omega^{-1}\,cm^2\,mol^{-1}$) of the solid complexes (table 1) is relatively low, indicating non-electrolytes [22]. The prepared solid complexes are characterized by IR, UV-Vis, ESR, and ^{1}H-NMR spectra, magnetic moment as well as thermal analysis (TGA).

3.2. *TGA of the complexes*

By thermal analysis, information on their properties, nature of intermediate and final products of their thermal decomposition can be obtained [23]. From TGA curves, the mass loss was calculated for the different steps and compared with those theoretically calculated for the suggested formulae based on the results of elemental analyses and MS as well as molar conductance measurements. TGA indicated the formation of metal oxide as the end product from which the metal content could be calculated and compared with that obtained from analytical determination. The found and calculated mass losses, relative residues and temperature observed in each step of TGA curves are given in table 2. The hydrated complexes decompose in four steps. The first step at 65–110°C is loss of water of crystallization; weight loss from 95 to 370°C is assigned to loss of coordinated water molecules. The third step at 210–395°C corresponds to removal of acetate as acetic acid, which is well known in the literature [24, 25]. The final decomposition step above 220°C includes complete evaporation of the ligand as well as formation of metal oxide as final product from which the metal content was found to be in very good agreement with the data obtained from EDTA titrations. Thermal degradation of **12**, as an example, is given as follows:

$$\left[Zn_3L^3(AcO)_3(H_2O)_3\right]\cdot 3H_2O \xrightarrow{52-85^\circ C} \left[Zn_3L^3(AcO)_3(H_2O)_3\right]$$

$$\left[Zn_3L^3(AcO)_3(H_2O)_3\right] \xrightarrow{120-150^\circ C} \left[Zn_3L^3(AcO)_3\right]$$

$$\left[Zn_3L^3(AcO)_3\right] \xrightarrow{160-210^\circ C} \left[Zn_3L^3\right]$$

$$\left[Zn_3L^3\right] \xrightarrow{220-795^\circ C} 3ZnO$$

Thus, the overall thermogravimetric results are consistent with the formulation of these complexes.

3.3. *IR spectra and mode of bonding*

Important IR spectral bands of the ligand and its complexes are shown in "Supplementary material" together with their assignments. The ligands contain different coordination sites. The ν(C=N) of azomethine at 1534–1530 cm^{-1} in the free ligands have obvious shifts after complexation, indicating coordination of azomethine nitrogen [4]. Bands of the free ligands at 1621–1609 and 3339–3216 cm^{-1} due to ν(C=O) and ν(NH), respectively, are shifted in spectra of **1**–**16** indicating participation of these groups in complex formation. The ligands exhibit two bands at 1324–1302 and 1179–1178 cm^{-1} due to $\nu_{as}(SO_2)$ and $\nu_s(SO_2)$ which are shifted upon complexation (Supplementary material). The shift of SO_2 stretching frequencies may be attributed to transformation of the sulfonamide (SO_2NH) to enol (SO(OH)N) as a result of complex formation to give more stable six-membered rings [6, 7]. The appearance of ν(OH), δ(OH), and γ(OH) at 3425–3407, 1138–1129, and 824–823 cm^{-1} in the free ligands confirm enolization of C=O. IR bands ($\nu(H_2O)$) of coordinated water at 3445–3397 cm^{-1} indicate binding of water to the metal. The presence of coordinated water renders it difficult to follow the behavior of the OH groups on complex formation from the stretching vibrations [6]. So far IR spectra of all the complexes, non-ligand bands at 567–517 and 467–406 cm^{-1} can be assigned to ν(M–O) and ν(M–N),

Table 2. TGA for most of the investigated complexes.

Compound No.	% Loss in weight found (Calcd)	Temperature range (°C)	Assignment (thermal process)
1	10.88 (10.41)	80–110	Loss of four coordinated H_2O
	5.00 (5.20)	200–240	Removal of two coordinated H_2O
	17.56 (17.06)	250–280	Evaporation of two acetate groups as acetic acid molecules [24, 25]
	30.00 (29.73.25)	300–795	Decomposition of the ligand and formation of metal oxide
2	15.00 (14.79)	200–250	Removal of two coordinated H_2O
	14.82 (15.37)	270–470	Decomposition of the ligand and formation of metal oxide
3	15.00 (15.44)	200–320	Removal of six coordinated H_2O
	17.00 (16.88)	330–390	Evaporation of two acetate groups as acetic acid molecules [24, 25]
	21.30 (21.34)	4000–795	Decomposition of the ligand and formation of metal oxide
5	7.54 (7.98)	75–113	Loss of five coordinated H_2O
	4.58 (4.79)	150–220	Removal of four coordinated H_2O
	15.88 (15.71)	250–292	Evaporation of three acetate groups as acetic acid molecules [24, 25]
	27.23 (29.73)	300–795	Decomposition of the ligand and formation of metal oxide
6	6.38 (5.94)	75–100	Loss of four hydrated H_2O
	13.62 (13.37)	200–320	Removal of nine coordinated H_2O
	15.00 (14.61)	325–345	Evaporation of three acetate groups as acetic acid molecules [24, 25]
	18.57 (18.53)	350–460	Decomposition of the ligand and formation of metal oxide
7	9.90 (9.96)	90–110	Loss of seven hydrated H_2O
	12.65 (12.81)	330–370	Removal of nine coordinated H_2O
	14.21 (13.99)	375–395	Evaporation of three acetate groups as acetic acid molecules [24, 25]
	17.76 (17.75)	400–650	Decomposition of the ligand and formation of metal oxide
8	3.26 (3.31)	50–96	Loss of two hydrated H_2O
	5.21 (4.97)	110–150	Removal of three coordinated H_2O
	16.52 (16.28)	170–245	Evaporation of three acetate groups as acetic acid molecules [24, 25]
	22.92 (22.48)	250–795	Decomposition of the ligand and formation of metal oxide
9	10.31 (10.78)	60–95	Loss of six coordinated H_2O
	5.69 (5.39)	210–235	Removal of three coordinated H_2O
	17.98 (17.66)	250–345	Evaporation of three acetate groups as acetic acid molecules [24, 25]
	30.81 (30.79)	350–795	Decomposition of the ligand and formation of metal oxide
10	5.88 (5.41)	80–98	Removal of four hydrated H_2O
	10.46 (10.82)	160–330	Evaporation of eight coordinated H_2O
	11.38 (11.25)	350–795	Decomposition of the ligand and formation of metal oxide
12	5.82 (5.51)	52–85	Loss of three hydrated H_2O
	5.26 (5.51)	120–150	Removal of three coordinated H_2O
	18.51 (18.07)	160–210	Evaporation of three acetate groups as acetic acid molecules [24, 25]
	25.21 (24.91)	220–795	Decomposition of the ligand and formation of metal oxide
13	10.13 (10.60)	60–110	Loss of one hydrated and five coordinated H_2O
	7.01 (7.07)	130–220	Removal of four coordinated H_2O
	17.32 (17.37)	230–360	Evaporation of three acetate groups as acetic acid molecules [24, 25]
	30.39 (30.35)	380–795	Decomposition of the ligand and formation of metal oxide
14	6.52 (6.67)	45–65	Loss of five hydrated H_2O
	10.98 (10.68)	220–280	Removal of eight coordinated H_2O
	10.88 (11.10)	300–795	Decomposition of the ligand and formation of metal oxide
15	16.21 (15.99)	250–330	Removal of nine coordinated H_2O.
	17.89 (17.47)	350–390	Evaporation of three acetate groups as acetic acid molecules [24, 25]
	22.10 (22.21)	400–500	Decomposition of the ligand and formation of metal oxide

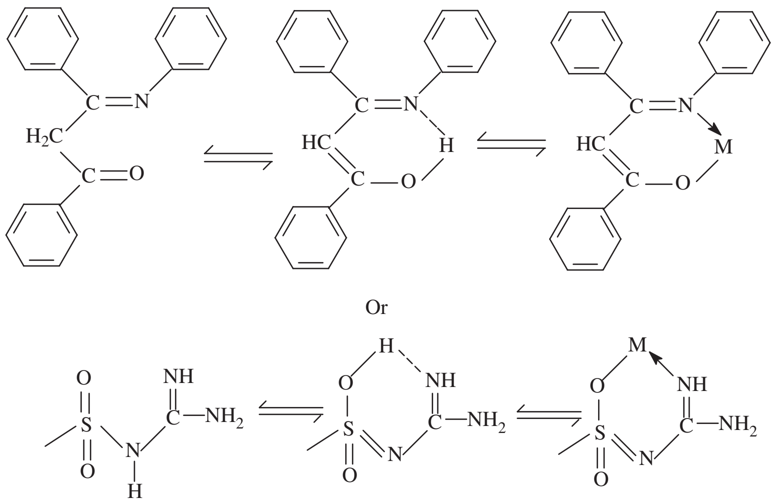

Scheme 1. Keto–enol toutmerism in ligands and modes of bonding in the formed complexes.

respectively [25–27]. IR spectra reveal that the ligands coordinate to metal *via* azomethine-N, enolic-OH of sulfonamide and enolic OH formed through a keto–enol tautomerism (of C=O group) in coordination (scheme 1) [6, 7, 27].

3.4. *Electronic, ESR spectra, and magnetic moment measurements*

The electronic absorption spectra of the chelates are studied as nujol mulls and DMF solution and compared with free ligand spectra (table 3). The shifts of the intra-ligand bands can be attributed to coordination to metal, while new bands (and change in color) of the complexes can be attributed to d–d transitions within the complexes [7, 27]. Electronic spectra of the Mn(II) complexes **1**, **5**, **9**, and **13** display two absorption bands with maximum absorption at 17,857–18,519 and 20,619–21,053 $\mathrm{cm^{-1}}$ as nujol mull (18,692–18,939 and 21,739–23,256 $\mathrm{cm^{-1}}$ in DMF solution), which are assigned to ${}^6T_{1g} \rightarrow {}^4A_{1g}(G)$ and ${}^6T_{1g} \rightarrow {}^4A_{2g}(D)$ transitions, respectively [7, 28, 29]. They have μ_{eff} values of 5.72–5.98 B.M which indicate octahedral geometry around Mn(II) [7, 28]. X-band ESR spectra of **1** and **5** measured at room temperature (300 K) display broad signals with no obvious hyperfine splitting, having g_{eff} values = 2.3241 and 2.4102, which confirm octahedral high spin Mn(II) complexes [25, 30]. Electronic spectra of Co(II) complexes **2**, **6**, **10**, and **14** have two bands at 16,529–18,182 and 20,534–21,505 as nujol mull (16,611–18,762 and 20,833–22,727 nm in DMF solution), assigned to ${}^4T_{1g}(F) \rightarrow {}^4T_{2g}(P)$ and ${}^4T_{1g}(F) \rightarrow {}^4A_{2g}(F)$ transitions [7, 31], respectively, indicating octahedral geometry around Co(II) [7, 31]. The magnetic moments (table 3) for **2**, **6**, **10**, and **14** are 4.73–4.88 B.M. confirming octahedral structures [25, 27, 32]. The X-band ESR spectra of **2** and **6** exhibit dissymmetric broad signals with g_{eff} values equal to 2.5029 and 2.5520, characteristic of Co(II) of octahedral structure [25, 33]. In **10** and **14**, H_3L^3 and H_3L^4 are bianionic ligands, so the stoichiometries of **10** and **14** indicate Co(II). All data for Co(II) complexes with O/N-ligands indicate octahedral high-spin paramagnetic ($3d^7$ system), which are well established in the literature [25, 33, 34].

Table 3. UV-Vis and ^{1}H-NMR spectral data as well as magnetic moment values of the complexes.

Compound No.	Electronic spectra (ν in cm^{-1})		Intra-ligand transition (ν cm^{-1})	μ_{eff}	^{1}H-NMR signals					
	Nujol mull	DMF			δ_{OH}	δ_{Ar}	δ_{NH}	δ_{NH_2}	δ_{CH_2}	δ_{CH_3}
H_2L^1			26,178		8.00	7.39–7.36	6.54	5.67	4.11	2.49
1	18,519 and 21,053	18,868 and 23,256	25,974	5.98		7.36–7.32	6.52	5.65	3.69	2.49
2	16,529 and 21,053	16,611 and 22,727	25,974	4.82		7.38–7.34	6.55	5.61	3.40	2.49
3	16,667 and 21,739	16,529 and 22,222	26,110	3.14		7.36–7.33	6.53	5.65	3.38	2.49
4	18,182	17,857	26,042	d		7.38–7.35	6.53	5.65	3.42	2.49
H_2L^2	–	–	26,667	–	8.31	7.66–7.54	6.93	–	3.45	
5	17,857 and 20,833	18,692 and 22,222	25,000	5.72	–	–	–	–	–	–
6	18,182 and 21,505	16,667 and 20,833	25,641	4.73	–	–	–	–	–	–
7	15,152 and 22,222	15,385 and 22,727	25,974	3.32	–	–	–	–	–	–
8	18,868	17,544	26,316	d	–	7.49–7.47	6.76		3.38	
H_2L^3			25,000	–	8.08	7.85–7.55	6.65			3.40
9	18,182 and 20,619	18,762 and 21,739	24,691	5.87	–	7.84–7.41	6.01			3.38
10	17,857 and 20,534	18,416 and 21,505	24,390	4.88	–	7.84–7.42	6.02			3.33
11	17,544 and 20,833	18,182 and 21,368	24,631	3.01	–	7.84–7.41	6.02			3.39
12	18,018	17,668	24,510	d	–	–	–	–	–	–
H_2L^4	–	–	23,256	–	–	7.85–7.52	6.61	–	–	3.41
13	18,315 and 20,790	18,939 and 21,834	23,095	5.80	–	7.65–7.11	6.53	–	–	3.36
14	17,921 and 20,619	18,762 and 21,692	22,989	4.79	–	7.54–7.09	6.54	–	–	3.36
15	17,668 and 20,921	18,519 and 21,645	22,833	3.31	–	7.49–7.08	5.88			3.08
16	18,349	17,986	23,148	d	–	–	–	–	–	–

μ_{eff} = magnetic moment (B.M.); d = diamagnetic; — = not measured.

The high g_{eff} values, dissymmetry, and broadness of the signals for **1**, **2**, **5**, and **6** indicate strong magnetic, i.e. obvious spin-exchange, metal–metal interactions [35]. The positive contribution in g_{eff} values (table 3) over that of the free electron ($g_{\mathrm{eff}} = 2.0023$) may indicate an increase in covalent bonding between the metal ions and the ligand molecule [36]. The nujol mull (DMF) electronic spectra of Ni(II) complexes **3**, **7**, **11**, and **15** show two bands at 15,152–17,668 (15,385–18,519) and 20,833–22,222 (21,368–22,727) cm^{-1}, assigned to $^3A_{2g} \rightarrow {}^3T_{1g}(F)$ and $^3A_{2g} \rightarrow {}^3T_{1g}(P)$ transitions [7, 25, 37]. Magnetic moment values of Ni(II) complexes (table 3) fall within the 3.01–3.31 range normally observed for octahedral Ni(II) complexes [27, 32]. Electronic spectra of **4**, **8**, **12**, and **16** as nujol mull (DMF) displayed CT bands at 18,018–18,868 (17,544–17,986) cm^{-1} ($L \rightarrow M$) [38]. Zn(II) complexes are diamagnetic as expected.

3.5. *^{1}H-NMR spectra*

The ^{1}H-NMR spectra of complexes are studied and free ligands (table 3) help determine the center of chelation and the replaceable hydrogens on complex formation. The signals at 7.85–7.32, 6.93–6.50, and 5.67 due to δ_{Ar}, δ_{NH} and $\delta_{\mathrm{NH_2}}$ in the free ligand spectra shift downfield in spectra of the complexes due to increased conjugation on coordination, supporting coordination of ligands to metal [39]. Signals at 8.00, 8.31, and 8.08 ppm due to δ_{OH} in spectra of H_2L^1, H_3L^2, and H_3L^3, respectively, support the presence of OH produced from keto–enol tautomerism. ^{1}H-NMR spectra of the complexes do not show a signal which could be assigned to OH denoting that complex formation occurs *via* deprotonation of these groups [40, 41]. ^{1}H-NMR spectra of the complexes support the conclusions derived from IR and UV-Vis spectra (scheme 1). Similar viewpoints have been advanced by Wang and Ma [39] and Chaudhry *et al.* [41] in their reports on paramagnetic Cu(II) complexes [39] and diamagnetic Zr(IV) complexes [41], respectively.

4. Structural interpretation and conclusion

Although many articles have been published on metal ion complexes of Schiff bases derived from sulfa drugs due to their biological activity and wide applications in pharmaceutical sciences, most dealt with mononuclear metal complexes [3–7]. For example, Anacona *et al.* [42] reported the synthesis, crystal structure and superoxide dismutase mimetic activity of [pyrrolidinium][Co(sulfathiazole)3(pyrrolidine)]. Li *et al.* [43] studied the crystal structures and characterization of two mononuclear Cu(II) complexes with *N*-[2-(2-hydroxybenzylideneamino)propyl]-4-methylbenzenesulfonamide and *N*-[2-(2-hydroxybenzylidene-amino)phenyl]-4-methylbenzenesulfonamide. We reported preparation and characterization of some sulfa-guanidine Schiff base derivatives [17] and their binuclear complexes [44]. Our goal is to increase the number of metal nuclei present in such complexes to increase their potential activity in applications, such as medical prevalence [3], electron transfer and nitrogen fixing enzymes [45], catalysis and material science [12–14]. So, in this article we extend our research on preparation and characterization of trihomonuclear Mn(II), Co(II), Ni(II), and Zn(II) complexes with some sulfa-guanidine Schiff bases used previously [17, 44]. Metal complexes of such type are of interest especially due to their potential as biocides and nematicides with electrical and magnetic properties [46].

The structures proposed are based on octahedral or tetrahedral geometries and the ligands coordinate to the metal ions *via* azomethine-N, enolic-OH of sulfonamide group and enolic OH formed through a keto–enol tautomerism of C=O groups in the coordination centers. Conductance data reveal that the complexes are non-electrolytes. The thermal data confirm the suggested formula, based on elemental analyses (C, H, N, and M) and MS. According to the above data, the structure of the complexes is given in figure 2.

References

[1] A. Bult. In *Metal Ions in Biological Systems*, H. Sigel (Ed.), Marcel Dekker, New York (1983).
[2] Th. Nogrady. *Medicinal Chemistry*, 2nd Edn, Oxford University Press, New York (1988).
[3] P. Nagaraja, K.R. Sunitha, R.A. Vasantha, H.S. Yathirajan. *Eur. J. Pharm. Biopharm.*, **53**, 187 (2002).
[4] R.C. Maurya, P. Patel. *Synth. React. Inorg. Met.-Org. Chem.*, **33**, 801 (2003).
[5] R.C. Maurya, S. Rajput. *J. Mol. Struct.*, **794**, 24 (2006).
[6] G.G. Mohamed, M.A.M. Gad-Elkareem. *Spectrochim. Acta, Part A*, **68**, 1382 (2007).
[7] C.M. Sharaby. *Spectrochim. Acta, Part A*, **66**, 1271 (2007).
[8] R.M. Issa, A.M. Khedr, A. Tawfik. *Synth. React. Inorg. Met.-Org. Chem.*, **34**, 1087 (2004).
[9] T.M. Ismail, A.M. Khedr, S.M. Abu-El-Wafa, R.M. Issa. *J. Coord. Chem.*, **57**, 1179 (2004).
[10] K. Selmeczi, M.G. Speier, E. Farkas, M. Réglier. *Eur. J. Inorg. Chem.*, 1022 (2006).
[11] J. Du, X. Meng, X. Zeng. *Chin. J. Chem.*, **26**, 421 (2008).
[12] S. Albedyhl, M.T. Averbuch-Pouchot, C. Belle, B. Krebs, J.L. Pierre, E. Saint-Aman, S. Torelli. *Eur. J. Inorg. Chem.*, 1457 (2001).
[13] X. Chen, X. Peng, J. Wang, Y. Wang, S. Wu, L. Zhang, T. Wu, Y. Wu. *Eur. J. Inorg. Chem.*, 5400 (2007).
[14] H. Ngyen, M. Orlamuender, D. Pretzel, I. Agricola, U. Sternberg, S. Reissmann. *J. Pept. Sci.*, **14**, 1010 (2008).
[15] H.D. Saw. *J. Am. Chem. Soc.*, **101**, 154 (1967).
[16] A.I. Vogel. *A Text Book of Quantitative Inorganic Analysis*, Longmans, London (1969).
[17] H. Mattapalli, W.B. Monteith, C.S. Burns, A.S. Danell, *J. Am. Soc. Mass Spectr.*, **20**, 199 (2009).
[18] S.S. Kandil, S.M.A. Katib, N.H.M. Yarkandi. *Transition Met. Chem.*, **32**, 791 (2007).
[19] B.K. Singh, P. Mishra, B.S. Garg. *Transition Met. Chem.*, **32**, 603 (2007).
[20] B.J. Aylett. *The Chemistry of Zinc, Cadmium and Mercury: Comprehensive Inorganic Chemistry*, pp. 187–308, Pergamon Press, Oxford (1975).
[21] J.K.S. Moller, C.E. Adamsen, R.R. Catharino, L.H. Skibsted, M.N. Eberlin. *Meat Sci.*, **75**, 203 (2007).
[22] W.J. Geary. *Coord. Chem. Rev.*, **7**, 81 (1971).
[23] M. Badea, A. Emandi, D. Marinescu, E. Cristurean, R. Olar, A. Braileanu, P. Budrugeac, E. Segal. *J. Therm. Anal. Calorim.*, **72**, 525 (2003).
[24] R.M. Issa, S.A. Amer, I.A. Mansour, A.I. Abdel-Monsef. *J. Therm. Anal. Cal.*, **90**, 261 (2007).
[25] K.Y. El-Baradie. *Monatsh. Chem.*, **136**, 1139 (2005).
[26] J.R. Ferraro. *Low Frequency Vibrations of Inorganic and Coordination Compounds*, 1st Edn, Plenum Press, New York (1971).
[27] C.M. Sharaby. *Spectrochim. Acta, Part A*, **62**, 326 (2005).
[28] F.A. Cotton, G. Wilkinson, C.A. Murillo, M. Bochmann. *Advanced Inorganic Chemistry*, 6th Edn, Wiley, New York (1999).
[29] S. Chandra, S.D. Sharma. *Transition Met. Chem.*, **27**, 732 (2002).
[30] R.S. Drago. *Physical Methods in Chemistry*, Saunders, Philadelphia, PA (1977).
[31] A.B.P. Lever. *Inorganic Electronic Spectroscopy*, 2nd Edn, Elsevier, Amsterdam (1984).
[32] A.I. Vogel. *Quantitative Inorganic Analysis Including Elemental Instrumental Analysis*, 2nd Edn, Longmans, London (1962).
[33] S.M. Abu-Elwafa, N.A. El-Wakiel, R.M. Issa, R.A. Mansour. *J. Coord. Chem.*, **58**, 683 (2005).
[34] B. Singh, K.K. Narang, R. Srivastava. *Synth. React. Inorg. Met.-Org. Chem.*, **32**, 1561 (2002).
[35] A. Bencini, C. Benelli, A. Caneschi, R.L. Carlin, A. Dei, D. Gatteschi. *J. Am. Chem. Soc.*, **107**, 8128 (1985).
[36] I. Fidone, K.W.H. Stevens. *Proc. Phys. Soc. (London)*, **37**, 116 (1957).
[37] M. Kondo, N. Kuob. *J. Phys. Chem.*, **62**, 1558 (1958).

[38] N.R.S. Kumar, M. Nethiji, K.C. Patil. *Polyhedron*, **10**, 365 (1991).
[39] B. Wang, H. Ma. *Synth. React. Inorg. Met.-Org. Chem.*, **34**, 1009 (2004).
[40] J. Knoeck, J.A. Buchholz. *Talanta*, **18**, 895 (1971).
[41] S.C. Chaudhry, C. Verma, S.S. Bhatt, N. Sharma. *Synth. React. Inorg. Met.-Org. Chem.*, **34**, 1031 (2004).
[42] J.R. Anacona, D. Lorono, M. Azocar, R. Atencio. *J. Coord. Chem.*, **62**, 951 (2009).
[43] S. Li, Q. Zhai, M. Hu, Y. Jiang. *J. Coord. Chem.*, **62**, 2709 (2009).
[44] R.M. Issa, S.A. Atyia, A.M. Khedr, D.F. Draz. *J. Coord. Chem.*, **62**, 1859 (2009).
[45] C.Y. Wu, L.H. Chen, W.S. Hwang, H.S. Chen, H.S. Chen, C.H. Hung. *J. Organomet. Chem.*, **689**, 2192 (2004).
[46] M. Jain, S. Gaur, V.P. Singh, R.V. Singh. *Appl. Organomet. Chem.*, **18**, 73 (2004).